Published in final edited form as:
J Mol Cell Cardiol. 2013 March ; 56: 44–54. doi:10.1016/j.yjmcc.2012.12.003.

Tetrahydrobiopterin improves diastolic dysfunction by reversing changes in myofilament properties

Euy-Myoung Jeong[a,1], **Michelle M. Monasky**[b,1], **Lianzhi Gu**[a], **Domenico M. Taglieri**[b], **Bindiya G. Patel**[b], **Hong Liu**[a], **Qiongying Wang**[a], **Ian Greener**[a], **Samuel C. Dudley Jr.**[a], and **R. John Solaro**[b,*]

[a] Department of Medicine, Section of Cardiology, College of Medicine, University of Illinois at Chicago, Chicago, IL, USA

[b] Department of Physiology and Biophysics and Center for Cardiovascular Research, College of Medicine, University of Illinois at Chicago, Chicago, IL, USA

Abstract

Despite the increasing prevalence of heart failure with preserved left ventricular function, there are no specific treatments, partially because the mechanism of impaired relaxation is incompletely understood. Evidence indicates that cardiac relaxation may depend on nitric oxide (NO), generated by NO synthase (NOS) requiring the co-factor tetrahydrobiopterin (BH_4). Recently, we reported that hypertension-induced diastolic dysfunction was accompanied by cardiac BH_4 depletion, NOS uncoupling, a depression in myofilament cross-bridge kinetics, and S-glutathionylation of myosin binding protein C (MyBP-C). We hypothesized that the mechanism by which BH_4 ameliorates diastolic dysfunction is by preventing glutathionylation of MyBP-C and thus reversing changes of myofilament properties that occur during diastolic dysfunction. We used the deoxycorticosterone acetate (DOCA)-salt mouse model, which demonstrates mild hypertension, myocardial oxidative stress, and diastolic dysfunction. Mice were divided into two groups that received control diet and two groups that received BH_4 supplement for 7 days after developing diastolic dysfunction at post-operative day 11. Mice were assessed by echocardiography. Left ventricular papillary detergent-extracted fiber bundles were isolated for simultaneous determination of force and ATPase activity. Sarcomeric protein glutathionylation was assessed by immunoblotting. DOCA-salt mice exhibited diastolic dysfunction that was reversed after BH_4 treatment. Diastolic sarcomere length (DOCA-salt 1.70±0.01 vs. DOCA-salt+BH_4 1.77±0.01 μm, $P<0.001$) and relengthening (relaxation constant, τ, DOCA-salt 0.28±0.02 vs. DOCA-salt+BH_4 0.08±0.01, $P<0.001$) were also restored to control by BH_4 treatment. pCa_{50} for tension increased in DOCA-salt compared to sham but reverted to sham levels after BH_4 treatment. Maximum ATPase rate and tension cost (ΔATPase/ΔTension) decreased in DOCA-salt compared to sham, but increased after BH_4 treatment. Cardiac MyBP-C glutathionylation increased in DOCA-salt compared to sham, but decreased with BH_4 treatment. MyBP-C glutathionylation correlated with the presence of diastolic dysfunction. Our results suggest that by depressing S-glutathionylation of MyBP-C, BH_4 ameliorates diastolic dysfunction by reversing a decrease in cross-bridge turnover kinetics.

* Corresponding author at: Department of Physiology and Biophysics, (M/C 901), College of Medicine, University of Illinois, 835 S. Wolcott Ave, Chicago, IL 60612-7342, USA. Tel.: +1 312 996 7620; fax: +1 312 996 1414. solarorj@uic.edu. .
[1]These authors contributed equally to this work.

Disclosure statement S.C.D.: patents pending titled, "Methods and Compositions for Treating Diastolic Dysfunction (#11/895,883)", "Glutathionylated Myosin Binding Protein C (MyBP-C) as a Biomarker of Diastolic Heart Failure (#61/544,030 and #61/618,900)" and "Methods of Diagnosing Diastolic Dysfunction (PCT/US2010/54096)".

Appendix A. Supplementary data Supplementary data to this article can be found online at http://dx.doi.org/10.1016/j.yjmcc.2012.12.003.

These data provide evidence for modulation of cardiac relaxation by post-translational modification of myofilament proteins.

Keywords

Deoxycorticosterone acetate (DOCA)-salt; mice; Diastolic heart failure; Oxidative stress; Ca^{2+} sensitivity; MyBP-C; S-glutathionylation

1. Introduction

Hypertension is the most common risk factor for diastolic dysfunction in humans, which can lead to heart failure with preserved ejection fraction [1]. This type of heart failure is increasing, and accounts for significant mortality and healthcare expenditures [1,2]. Current treatments for diastolic dysfunction are inadequate, partially because the mechanism of altered myocardial relaxation is incompletely understood [3]. Nitric oxide (NO) generated by NO synthase (NOS) is a critical modulator of cardiac relaxation [4], and NO bioavailability is regulated by tetrahydrobiopterin (BH_4) [5].

Under physiological conditions, NOS catalyzes the production of NO from L-arginine to modulate myofilament contractility through mechanisms that are not clear [6–9]. BH_4 depletion, leads to NOS uncoupling [5,10], the production of superoxide instead of NO, and diastolic dysfunction [5,11]. BH_4 supplementation reverses these effects. Recently, we have reported that diastolic dysfunction was characterized by altered myofilament properties and by S-glutathionylation of cardiac myosin binding protein-C (MyBP-C) [12]. S-glutathionylationis an oxidative post-translational modification of protein cysteines by the addition of the anti-oxidant tripeptide glutathione [13–15]. We tested whether the improvement in diastolic dysfunction with BH_4 treatment correlated with changes in myofilament properties and in S-glutathionylation of cardiac MyBP-C.

We demonstrate that oral administration of BH_4 improves diastolic dysfunction, reverses the changes in actin-myosin cross-bridge cycling, and decreases S-glutathionylated MyBP-C. Our results support the hypothesis that oxidative post-translational modifications and associated modulation of myofilament properties is a molecular mechanism for diastolic dysfunction.

2. Methods

All protocols were in accordance with the guidelines of the Animal Care and Use Committee of the University of Illinois and comply with the laws of the United States of Ameria.

2.1. Generation of DOCA-salt mouse model

Previously, we have shown that the DOCA-salt mouse model leads to mild hypertension, NOS uncoupling, myocardial oxidative stress, and diastolic dysfunction [10]. A gradual and mild elevation in blood pressure was induced by unilateral nephrectomy, subcutaneous implantation of a controlled release deoxycorticosterone acetate (DOCA) pellet (0.7 mg/d; Innovative Research of America, Sarasota, FL), and substituting drinking water with 1.05% saline. Control animals underwent a sham operation, had placebo pellet implantation, and received water without salt.

2.2. Administration of BH_4

Mice were divided into two groups which received a control diet (sham N=7; DOCA-salt N=10) and two groups which received a BH_4 supplemental diet of 5 mg BH_4/day (200 mg/kg/day, Research Diets Inc, New Brunswick, NJ; sham+BH_4 N=8; DOCA-salt+BH_4 N=8). The supplemental diet began on day 11 after surgery, and continued until day 18, when the mice were analyzed and sacrificed.

2.3. Transthoracic echocardiography

Mitral pulse wave Doppler flow and tissue Doppler imaging (TDI) were performed using the Vevo 770 high-resolution in vivo imaging system (Visual Sonics, Toronto, Canada) [10]. Mice were anesthetized with 1–1.5% isoflurane until a heart rate of around 350–390 beats/min was achieved because measures of diastolic function are sensitive to heart rate and loading conditions. M-mode images in the parasternal long axis and the left ventricle (LV) short-axis views at the mid-papillary level were taken. Measurements were averaged from five consecutive beats during expiration. The images for each mouse were recorded for at least 5 s (30–40 cardiac cycles) from which three to five representative cycles with the highest quality imaging were selected. Percent fractional shortening (%FS) was calculated as 100×(LVEDd)—(LVESd)/(LVEDd) and percent LV ejection fraction (%EF) was calculated as $100\times[(7/2.4+LVEDd)\times LEDd^3]—[(7/2.4+LVESd)\times LVESd^3]/[(7/2.4+LVEDd)\times LEDd^3]$. Doppler measurements were made at the tips of the mitral leaflets for diastolic filling profiles in the apical four-chamber view. Mitral inflow velocities, peak early (E) and late (A) were measured by conventional pulsed-wave Doppler. TDI was used to determine the mitral annulus longitudinal velocities (Sm, E', and A') [10]. Baseline images before treatment were acquired to confirm diastolic dysfunction in DOCA-salt mice. Subsequently, the mice were fed with BH_4, followed by echocardiography at day 18.

2.4. Cardiomyocyte studies

Ventricular myocytes were isolated as previously described [10]. Hearts were excised from anesthetized mice, perfused with buffer (in mmol/L: NaCl 113, KCl 4.7, Na_2HPO_4 0.6, KH_2PO_4 0.6, $MgSO_4$ 1.2, Phenol Red 0.032, $NaHCO_3$ 12, $KHCO_3$ 10, HEPES 10, Taurine 30, 2-3-butanedione monoxime 10) and digested with collagenase II (Worthington Biochemical Co. Lakewood, NJ) for 7–8 min with 37 °C perfusion. Cardiomyocytes were washed with control buffers (in mmol/L: NaCl 133.5, KCl 4, Na_2HPO_4 1.2, HEPES 10, $MgSO_4$ 1.2 and 0.1% Bovine serum albumin) with serially increasing Ca^{2+} concentrations (0.2, 0.5, and 1 mmol/L). Then, myocytes were maintained in MEM medium (modified Eagle's medium with 1% insulin-transferrin-selenium, 0.1% bovine serum albumin, 1% glucose, and 1% penicillin/streptomycin) in a 95% O_2/5% CO_2 incubator at 37 °C until use.

The mechanical properties of the cardiomyocytes were assessed using an IonOptix Myocam System (IonOptix Inc., Milton, MA) as described previously [12]. Unloaded cardiomyocytes isolated from each group of mice were placed on a glass slide and allowed to adhere for 5 min, then imaged with an inverted microscope and perfused with a normal Tyrode's buffer (in mmol/L: 133 NaCl, 5.4 KCl, 5.3 $MgCl_2$, 0.3 Na_2PO_4, 20 HEPES, 10 glucose, pH 7.4) containing 1.2 mmol/L calcium at 37 °C with a temperature controller. Cardiomyocytes were paced with 10 V, 4 ms square wave pulses at 1.0 Hz, and sarcomere shortening and relengthening were assessed using the following indices: diastolic sarcomere length (SL, μm), peak fractional shortening (FS, %), the prolonged relaxation time constant τ ($a_0+a_1e^{t/\tau}$, t=time, s), relengthening time (s), and maximum relaxation velocity (dL/dt, μm/s).

2,3-Butanedione monoxime (BDM), a cross-bridge inhibitor, was used to measure residual sarcomere length. BDM inhibits the Ca^{2+} regulated attachment of the cross-bridges and force-generation of the attached cross-bridges [16]. Isolated single myocytes were loaded on

a chamber and perfused with BDM (10 mM) in Tyrode's solution at 37 °C. Sarcomere length was again measured while the myocytes were field-stimulated as described above.

2.5. Dissection of left ventricular papillary muscles and preparation of skinned fibers

Mice were anesthetized with pentobarbital (50 mg/kg IP), and the hearts were rapidly excised and rinsed in ice-cold relaxing solution (pH 7.0) composed of (in mM) 10 EGTA, 41.89 K-Prop, 6.57 $MgCl_2$, 100 BES, 6.22 ATP, 5 Na azide, and 10 creatine phosphate. The solution also contained 1 μg/mL leupeptin, 2.5 μg/ml pepstatin A, and 50 μM phenylmethylsulfonyl fluoride. Left ventricular papillary muscles were dissected and fiber bundles were prepared as previously described [17]. The fiber bundles were extracted overnight in relaxing solution plus 1% Triton X-100 at 4 °C.

2.6. Simultaneous determination of force and ATPase activity in detergent-extracted cardiac fiber bundles

Force and ATPase rate were measured simultaneously as previously described [17] using an experimental apparatus also previously described [18]. The fiber bundles were mounted between a force transducer and displacement motor using aluminum T-clips, and the sarcomere length was set to 2.2 μm using He–Ne laser diffraction [19]. The width and diameter were each measured at three points along the fiber bundle. Force per cross-sectional area was used to determine tension. The fiber was initially contracted at a saturating calcium concentration (pCa 4.5) and sarcomere length was again adjusted to 2.2 μm. Sarcomere length remained constant throughout the rest of the experiment.

ATPase activity was measured at 20 °C as previously described[17,20] and calibrated with rapid injections of ADP (0.5 nmol) with a motor-controlled syringe. The fiber was placed in relaxing solution for 2 min, then in the pre-activation solution for 2–3 min each time before being placed in the activating solution for 1–2 min (until stabilization of force) and then quickly returned to the relaxing solution. Various contraction–relaxation cycles were carried out using different ratios of total calcium concentration to total EGTA concentration. The final contraction was again at pCa 4.5.

2.7. Analysis of sarcomeric protein phosphorylation

In one series of experiments, we employed Pro-Q Diamond (Invitrogen) gel stain to determine changes in phosphorylation of myofilament proteins. We also employed site specific antibodies for MyBP-C (anti-phospho-peptide-Ser282) and for cTnI (anti-phopho-Ser23/Ser24). Detailed methods are presented in the Supplementary material.

2.8. Analysis of sarcomeric protein glutathionylation by western immunoblotting

Myofibrils were prepared from DOCA-salt and sham model hearts, and pellets were solubilized in a non-reducing 2× Laemmli buffer (4% SDS, 20% glycerol, 0.004% bromophenol blue, and 0.125 M Tris HCl pH 6.8). 25 mM N-ethylmaleimide (NEM) was added to the standard rigor buffer with Triton X-100, the standard rigor wash buffer and the 2× Laemmli buffer [21]. Using the protein concentration determined from an RC-DC (Bio-Rad) assay, 40 μg of total protein was applied to a 12% SDS-PAGE gel and transferred onto a 0.2 μm PVDF membrane. The blot was blocked in 5% nonfat dry milk with 2.5 mM NEM for 1 h. Anti-glutathione mouse monoclonal primary antibody (Virogen) was used at 1:1000 dilution along with anti-mouse HRP-conjugated secondary antibody (Sigma) at 1:100,000 dilution to detect for S-glutathionylation [22]. Optical density of the bands was measured with ImageQuant TL (GE Healthcare) and exported to Excel for further analysis.

2.9. Statistical analysis

Echocardiography, sarcomere shortening, skinned fiber tension, and ATPase measurements, as well as post-translational modifications of myofilament proteins, were statistically analyzed by two-way ANOVA followed by student's *t* test using JMP statistical software. Analysis of the relation between Ca^{2+} and tension or ATPase activity was fitted using a modified Hill equation as described previously [20]. Analysis of the relation between MyBP-C glutathionylation and echocardiographic, E/E' ratio was correlated in linear regression analysis. A value of $P<0.05$ was considered significantly different. Data are presented as means±SEM.

3. Results

3.1. Improvement in diastolic function with BH_4

Ten days after surgery, we employed echocardiography to characterize the diastolic dysfunction. Treatment with a BH_4 supplemental diet was begun on post-operative day 11, and echocardiography was repeated on postoperative day 18. The results can be seen in Fig. 1 and Table 1. Seven days of BH_4 administration in sham and DOCA-salt mice did not affect LV ejection fraction (Fig. 1A) or fractional shortening (Fig. 1B).

Mitral Doppler flow was measured at comparable heart rates (~average 370 beats/min) in all mice [10]. As we have reported in this model, mitral E velocity, A velocity, and the E/A ratio were not significantly changed in all groups (Figs. 1C and F). Nevertheless, mitral tissue Doppler E' was significantly decreased in the DOCA-salt mice indicating a pseudo-normal diastolic dysfunction stage. The ratio of E'/A' was significantly decreased in DOCA-salt mice and restored with BH_4 treatment (DOCA-salt+BH_4, 1.12±1.10 vs. DOCA-salt, 0.74±0.05, $P<0.05$). The sham and sham+BH_4 groups did not show any significant differences in E'/A' (Figs. 1D and G). The E/E' ratio, a measure of left atrial pressure, was significantly increased in DOCA-salt mice, and restored to the control level after BH_4 administration (Fig. 1E, DOCA-salt+BH_4, 34.5±2.2 vs. DOCA-salt, 43.7±2.7, $P<0.05$).

3.2. Improvement in cardiomyocyte parameters of relaxation with BH_4

To confirm diastolic relaxation impairment in the model, we isolated single myocytes from each group and measured sarcomeric contraction and relaxation function, as seen in Fig. 2. Diastolic sarcomere length was shortened in DOCA-salt mice (1.70±0.01 μm) and restored after BH_4 treatment (1.77±0.01 μm, $P<0.05$) (Figs. 2,A–D). Fractional shortening was not changed in all groups (Fig. 2C). On the other hand, the relaxation constant, τ (0.28±0.02 s), and 50% relengthening time (0.44±0.01 s) were significantly increased in DOCA-salt mice and returned to their normal levels after BH_4 treatment (τ, 0.08±0.01 s, $P<0.05$; 50% relengthening time, 0.24±0.01 s, $P<0.05$, Figs. 2E–F). The reduced relaxation rate in DOCA-salt mice (1.60±0.15 μm/s) reverted to control levels with BH_4 treatment (2.39±0.18 μm/s, $P<0.05$ Figs. 2G–H).

To determine whether increased diastolic tension could be explained by active cross-bridge cycling, we treated the myocytes with BDM, a non-competitive inhibitor of active force-generation [16]. Treatment of isolated myocytes with BDM (10 mM) increased residual sarcomere length in the sham and DOCA-salt groups. Treatment of either group with BH_4 resulted in significant relaxation as measured by sarcomere length. After BH_4 treatment, BDM had no effect, suggesting that BH_4 facilitated cross-bridge dissociation (Fig. 2I).

3.3. Myofilament properties altered by BH_4

In order to assess the relation between myocardial diastolic dysfunction and changes in myofilament properties, we performed analysis of tension and ATPase activity in skinned

fiber preparations (Figs. 3 and 4). Our results indicate that tension cost (ΔATPase/Δtension) of skinned fibers from the DOCA-salt group (6.5±0.2) was significantly ($P<0.05$) reduced compared to shams (8.5±0.3) demonstrating that a slowing of cross bridge kinetics was responsible for diastolic dysfunction. Tension cost in fibers from the DOCA-salt+BH_4 group was increased (7.4±0.4, $P<0.05$) compared to the DOCA-salt group to a level not significantly different from either sham group (Fig. 3 and Table 2).

Maximum ATPase rate was also significantly reduced in DOCA-salt mice. This was accompanied by modest changes in maximum tension, pCa_{50} for tension and ATPase rate. BH_4 treatment increased maximum tension and ATPase rates in both sham and DOCA-salt mice, again with modest changes in pCa_{50} and significant changes in tension cost that varied in DOCA-salt versus sham mice. (Fig. 4 and Table 2).

3.4. Myosin binding protein C post-translational modifications

In one set of experiments, we determined potential modifications in phosphorylation of myofilament proteins employing Pro-Q diamond phospho-protein gel stain (Fig. 5). With BH_4 treatment in the DOCA-salt mice, there was a decrease in phosphorylation of major myofilament proteins, MyBP-C, TnT3, cTnT4, and MLC2, but no change in cTnI phosphorylation. Phosphorylation of titin was increased in DOCA-salt mice, and restored by BH_4 treatment. The decreases in phosphorylation would tend to slow cross-bridge kinetics or increase diastolic stiffness, and thus are not likely to account for the reversal of effects of DOCA-salt on diastolic dysfunction with BH_4 treatment. To further test this conclusion, we determined the level of site-specific phosphorylation changes in both MyBP-C and cTnI (Supplemental Fig. 3). Phosphorylation at Ser282 of MyBP-C was decreased in myofilaments from hearts of DOCA-salt mice compared to shams. BH_4 further reduced phosphorylation of MyBP-C at Ser282 in myofilaments from DOCA-salt mice, but did not significantly alter phosphorylation at this residue in sham myofilaments. Phosphorylation of cTnI at Ser23/24 was significantly reduced in myofilaments from DOCA-salt mice compared to sham, but was not significantly changed by BH4 in either from DOCA-salt or sham mice. Decreases in phosphorylation of MyBP-C and TnI, have been previously demonstrated to slow cross-bridge kinetics [23,24]. Thus, one could speculate that the decrease in phosphorylation of these two proteins that we observe in hearts from DOCA-salt mice may contribute to the impaired relaxation. However, we did not observe a reversal of phosphorylation of these two proteins in the presence of BH4 when diastolic function had recovered. Therefore, our results indicate that while the lower phosphorylation MyBP-C and cTnI may play a role in diastolic dysfunction, changes in S-glutathionylation of MyBP-C correlate with changes in diastolic function mediated by BH_4 in this model (Fig. 5).

In view of our earlier findings indicating an increase in MyBP-C S-glutathionylation in cardiac myofilaments from DOCA-salt mice, we determined whether the BH_4 diet could reverse this modification. Representative gels and plotted data normalized to total protein loadings are shown in Fig. 6. MyBP-C glutathionylation was significantly increased in the DOCA-salt group compared to all other groups, which were not significantly different from each other. In the data shown in Fig. 7, we plotted diastolic function parameters (E/E' or E'/A' ratio) as a function of normalized MyBP-C glutathionylation. As shown in Figs. 7A and B, the E/E' ratio was significantly, positively correlated with MyBP-C glutathionylation (Slope=3.23±0.90, $R^2=0.305$, $^{**}P<0.01$). Moreover, TDI E'/A' ratio was negatively correlated with MyBP-C glutathionylation (Slope=−0.08±0.02, $R^2=0.257$, $^{**}P<0.01$). Myofilament tension cost was also inversely correlated with both MyBP-C glutathionylation and E/E' echocardiographic data. However, both phosphorylation levels of TnI and MyBP-C were not significantly correlated with tension cost (Figs. 7G–H).

4. Discussion

Results presented here provide new understanding of the role of cardiac myofilaments in the pharmacology and therapeutic efficacy of BH_4 for the treatment of diastolic dysfunction induced by pressure-overload. Overall, our results indicate that hypertension-associated diastolic dysfunction in this model likely arises mainly from a reduction in cross-bridge turnover kinetics and that administration of BH_4 results in amelioration of diastolic dysfunction by speeding these kinetics. Although correlative, our results support the hypothesis that changes in cross-bridge kinetics correlate with MyBP-C S-glutathionylation and that this oxidative modification may be responsible for the changes in cardiac dynamics. To the best of our knowledge, the present study is the first to report that treatment with BH_4 reduces increased levels of MyBP-C S-glutathionylation. Therefore, this post-translational modification may serve as a novel marker useful for the identification and treatment of diastolic heart dysfunction. Unlike in our previous study with ranolazine for treatment of diastolic dysfunction, BH4 reversed the glutathionylation of MyBP-C, suggesting that these two drugs work on the same disorder by different mechanisms, allowing for the possibility that the drugs could have additive or synergistic effects that need to be explored in future experiments [12].

Apart from our previous study indicating that S-glutathionylation correlated with changes in diastolic dysfunction and in tension cost, there is considerable evidence that modifications of MyBP-C affect diastolic function. Mutations in MyBP-C are known to induce diastolic dysfunction [25]. MyBP-C is also a substrate for multiple kinases, including protein kinase (PK)A, PKC, PKD, and CaMKII [26]. MyBP-C and its dephosphorylation have been shown to be associated with end stage human heart failure [27]. MyBP-C dephosphorylation has also been associated with its degradation [26,28–30], thick filament disruption, and contractile dysfunction [26,28,30]. Phosphorylation of MyBP-C by PKA accelerates cross-bridge turnover rates [26]. Interestingly, a non-PKA-phosphorylatable truncated mutant of MyBP-C (AIIP-:[t/t]) exhibited a dilated LV chamber diameter, increased septal thickness, and depressed systolic function. This model also exhibited significant diastolic dysfunction because of slower cross-bridge cycling in the absence of baseline phosphorylation of MyBP-C [31]. In general, our results fit with data in these studies indicating that effects of post-translational modifications in MyBP-C may be more prominently involved in altered cross-bridge kinetics and muscle dynamics than alterations in Ca-sensitivity. For example, employing loss of function models, Stelzer et al. reported that, in the intact myocardium, PKA phosphorylation of MyBP-C was a more prominent determinant of contraction and relaxation kinetics than phosphorylation of cardiac troponin I (cTnI), which was a more prominent determinant of Ca-sensitivity [32].

Nevertheless, in our experiments, MyBP-C phosphorylation did not correlate with diastolic dysfunction or BH_4 efficacy. In fact, compared to DOCA-salt myofilaments, the myofilaments from the DOCA-BH_4 treated hearts had reduced phosphorylation of MyBP-C as well as TnT, and MLC2. Yet BH_4 did not affect the phosphorylation of these proteins in the shams. A limitation of the study is that Pro-Q analysis measures total phosphorylation of a given protein, and MyBP-C contains multiple phosphorylation sites, the function of which is poorly understood. Thus, although we cannot exclude that site-specific phosphorylation may have contributed to diastolic dysfunction or the effect of BH_4, overall our data indicate that phosphorylation is not likely to contribute substantially to our findings of decreased tension cost and cross-bridge kinetics in the DOCA-salt myofilaments or to the amelioration of this effect with BH_4 treatment.

In addition to altered cross-bridge kinetics as a potential mechanism of diastolic dysfunction, modifications in sarcomeric diastolic function may be significantly affected by

modifications in titin [33,34]. In view of the potential modulation of extensibility by titin phosphorylation by protein kinase G [33,35], NO has been suggested to play an important role in regulating diastolic tone and ventricular filling through a cGMP-PKC dependent pathway [36]. Moreover, PKG activation has been suggested to affect the reduction of Ca^{2+} sensitivity through TnI phosphorylation at Ser23/24 and an increase in cross-bridge cycling rate, leading to acceleration of relaxation [37,38]. However, in the present study, both titin and TnI phosphorylation were not changed by BH_4 treatment in DOCA-salt mice suggesting another mechanism may be involved in the relaxation improvement via BH_4 in this model. Although our findings are novel with regard to effects of BH4 on the S-glutathionylation and functional effects of MyBP-C, there are potential limitations in its use. Moen et al. reported that the range of therapeutic efficacy of BH4 may be limited by its oxidation when administered orally [39].

An important issue is the molecular mechanism of the effect of S-glutathionylation on MyBP-C function. Possible mechanisms are couched in terms of current hypotheses as to how MyBP-C controls cross-bridge kinetics. One plausible mechanism is that the radial disposition of MyBP-C in relation to the thick filament proper is a determinant of the rates of entry of the cross-bridges into and out of the cross-bridge cycle. Proximity of cross-bridges has been demonstrated to be increased by PKA-dependent phosphorylation [40]. There is also evidence that MyBP-C directly interacts with actin in the thin filaments, and it is also plausible that modulation of thin filaments may result in increased cross-bridge kinetics [41]. Whatever the case, our data indicate that modification of one or more cysteine residues of MyBP-C under oxidative control by S-glutathionylation is likely to alter the proximity of the cross-bridges to or their interactions with the thin filament. In the case of the DOCA-salt model, the modification is maladaptive and induces a diastolic abnormality. It is interesting to speculate that oxidative modification of MyBP-C may also serve as an adaptive mechanism in homeostasis, which modulates cardiac relaxation reserve by controlling cross-bridge kinetics.

5. Conclusion

In summary, hypertension-induced diastolic dysfunction was characterized by reduced cross-bridge kinetics and tension cost that was reversed by BH_4. The effect of BH_4 correlated with glutathionylation of MyBP-C, suggesting that this post-translational modification may lead to diastolic dysfunction and that BH_4 treatment may work by preventing this oxidative modification.

Supplementary Material

Refer to Web version on PubMed Central for supplementary material.

Acknowledgments

The authors gratefully acknowledge Chad M. Warren for his valuable technical support.

Sources of funding This study was supported by NIH/NHLBI grants RO1 HL022231, RO1 HL064035, PO1 HL062426 to RJS, and NIH/NHLBI grants RO1 HL085558, RO1 HL073753, PO1 HL058000, and a Veterans Affairs MERIT grant to SCD. MMM was supported by NIH T32 HL07692-16-20; DMT was supported by a University of Illinois at Chicago Center for Clinical and Translational Science (Award Number UL1RR029879) from the National Center for Research Resources, and by a University of Illinois at Chicago Fellowship.

Abbreviations

A mitral inflow late filling velocity in pulse-wave Doppler

BDM	2,3-butanedione monoxime
BH_4	tetrahydrobiopterin
DOCA	deoxycorticosterone acetate
E	mitral inflow early filling velocity in pulse-wave Doppler
EF	ejection fraction
FS	fractional shortening
LV	left ventricle
MyBP-C	cardiac myosin binding protein-C
NEM	N-ethylmaleimide
NO	nitric oxide
NOS	nitric oxide synthase
PK	protein kinase
TDI	tissue Doppler imaging
cTnI	cardiac troponin I
TnT	troponin T

References

[1]. Schocken DD, Benjamin EJ, Fonarow GC, Krumholz HM, Levy D, Mensah GA, et al. Prevention of heart failure: a scientific statement from the American Heart Association Councils on Epidemiology and Prevention, Clinical Cardiology, Cardiovascular Nursing, and High Blood Pressure Research; Quality of Care and Outcomes Research Interdisciplinary Working Group; and Functional Genomics and Translational Biology Interdisciplinary Working Group. Circulation. 2008; 117:2544–65. [PubMed: 18391114]

[2]. Owan TE, Hodge DO, Herges RM, Jacobsen SJ, Roger VL, Redfield MM. Trends in prevalence and outcome of heart failure with preserved ejection fraction. N Engl J Med. 2006; 355:251–9. [PubMed: 16855265]

[3]. Ouzounian M, Lee DS, Liu PP. Diastolic heart failure: mechanisms and controversies. Nat Clin Pract Cardiovasc Med. 2008; 5:375–86. [PubMed: 18542106]

[4]. Ziolo MT, Kohr MJ, Wang H. Nitric oxide signaling and the regulation of myocardial function. J Mol Cell Cardiol. 2008; 45:625–32. [PubMed: 18722380]

[5]. Landmesser U, Dikalov S, Price SR, McCann L, Fukai T, Holland SM, et al. Oxidation of tetrahydrobiopterin leads to uncoupling of endothelial cell nitric oxide synthase in hypertension. J Clin Invest. 2003; 111:1201–9. [PubMed: 12697739]

[6]. Flesch M, Kilter H, Cremers B, Lenz O, Sudkamp M, Kuhn-Regnier F, et al. Acute effects of nitric oxide and cyclic GMP on human myocardial contractility. J Pharmacol Exp Ther. 1997; 281:1340–9. [PubMed: 9190870]

[7]. Prabhu SD, Azimi A, Frosto T. Nitric oxide effects on myocardial function and force-interval relations: regulation of twitch duration. J Mol Cell Cardiol. 1999; 31:2077–85. [PubMed: 10640437]

[8]. Ruetten H, Dimmeler S, Gehring D, Ihling C, Zeiher AM. Concentric left ventricular remodeling in endothelial nitric oxide synthase knockout mice by chronic pressure overload. Cardiovasc Res. 2005; 66:444–53. [PubMed: 15914109]

[9]. Ungureanu-Longrois D, Bezie Y, Perret C, Laurent S. Effects of exogenous and endogenous nitric oxide on the contractile function of cultured chick embryo ventricular myocytes. J Mol Cell Cardiol. 1997; 29:677–87. [PubMed: 9140825]

[10]. Silberman GA, Fan TH, Liu H, Jiao Z, Xiao HD, Lovelock JD, et al. Uncoupled cardiac nitric oxide synthase mediates diastolic dysfunction. Circulation. 2010; 121:519–28. [PubMed: 20083682]

[11]. Vasquez-Vivar J, Kalyanaraman B. Generation of superoxide from nitric oxide synthase. FEBS Lett. 2000; 481:305–6. [PubMed: 11041680]

[12]. Lovelock JD, Monasky MM, Jeong EM, Lardin HA, Liu H, Patel BG, et al. Ranolazine improves cardiac diastolic dysfunction through modulation of myofilament calcium sensitivity. Circ Res. 2012; 110:841–50. [PubMed: 22343711]

[13]. Adachi T, Weisbrod RM, Pimentel DR, Ying J, Sharov VS, Schoneich C, et al. S-Glutathiolation by peroxynitrite activates SERCA during arterial relaxation by nitric oxide. Nat Med. 2004; 10:1200–7. [PubMed: 15489859]

[14]. Adachi T, Pimentel DR, Heibeck T, Hou X, Lee YJ, Jiang B, et al. S-glutathiolation of Ras mediates redox-sensitive signaling by angiotensin II in vascular smooth muscle cells. J Biol Chem. 2004; 279:29857–62. [PubMed: 15123696]

[15]. Chen FC, Ogut O. Decline of contractility during ischemia-reperfusion injury: actin glutathionylation and its effect on allosteric interaction with tropomyosin. Am J Physiol Cell Physiol. 2006; 290:C719–27. [PubMed: 16251471]

[16]. Kagawa K, Horiuti K, Yamada K. BDM compared with P_i and low Ca^{2+} in the cross-bridge reaction initiated by flash photolysis of caged ATP. Biophys J. 1995; 69:2590–600. [PubMed: 8599666]

[17]. Wolska BM, Keller RS, Evans CC, Palmiter KA, Phillips RM, Muthuchamy M, et al. Correlation between myofilament response to Ca^{2+} and altered dynamics of contraction and relaxation in transgenic cardiac cells that express beta-tropomyosin. Circ Res. 1999; 84:745–51. [PubMed: 10205142]

[18]. de Tombe PP, Stienen GJ. Protein kinase A does not alter economy of force maintenance in skinned rat cardiac trabeculae. Circ Res. 1995; 76:734–41. [PubMed: 7728989]

[19]. de Tombe PP, ter Keurs HE. Force and velocity of sarcomere shortening in trabeculae from rat heart. Effects of temperature. Circ Res. 1990; 66:1239–54. [PubMed: 2335024]

[20]. Martin AF, Phillips RM, Kumar A, Crawford K, Abbas Z, Lessard JL, et al. Ca^{2+} activation and tension cost in myofilaments from mouse hearts ectopically expressing enteric gamma-actin. Am J Physiol Heart Circ Physiol. 2002; 283:H642–9. [PubMed: 12124211]

[21]. Layland J, Cave AC, Warren C, Grieve DJ, Sparks E, Kentish JC, et al. Protection against endotoxemia-induced contractile dysfunction in mice with cardiac-specific expression of slow skeletal troponin I. FASEB J. 2005; 19:1137–9. [PubMed: 15855227]

[22]. Hill BG, Ramana KV, Cai J, Bhatnagar A, Srivastava SK. Measurement and identification of S-glutathiolated proteins. Methods Enzymol. 2010; 473:179–97. [PubMed: 20513478]

[23]. Biesiadecki BJ, Kobayashi T, Walker JS, John SR, de Tombe PP. The troponin C G159D mutation blunts myofilament desensitization induced by troponin I Ser23/24 phosphorylation. Circ Res. 2007; 100:1486–93. [PubMed: 17446435]

[24]. Tong CW, Stelzer JE, Greaser ML, Powers PA, Moss RL. Acceleration of crossbridge kinetics by protein kinase A phosphorylation of cardiac myosin binding protein C modulates cardiac function. Circ Res. 2008; 103:974–82. [PubMed: 18802026]

[25]. Fraysse B, Weinberger F, Bardswell SC, Cuello F, Vignier N, Geertz B, et al. Increased myofilament Ca^{2+} sensitivity and diastolic dysfunction as early consequences of Mybpc3 mutation in heterozygous knock-in mice. J Mol Cell Cardiol. 2012; 52:1299–307. [PubMed: 22465693]

[26]. Barefield D, Sadayappan S. Phosphorylation and function of cardiac myosin binding protein-C in health and disease. J Mol Cell Cardiol. 2010; 48:866–75. [PubMed: 19962384]

[27]. El-Armouche A, Pohlmann L, Schlossarek S, Starbatty J, Yeh YH, Nattel S, et al. Decreased phosphorylation levels of cardiac myosin-binding protein-C in human and experimental heart failure. J Mol Cell Cardiol. 2007; 43:223–9. [PubMed: 17560599]

[28]. Decker RS, Decker ML, Kulikovskaya I, Nakamura S, Lee DC, Harris K, et al. Myosin-binding protein C phosphorylation, myofibril structure, and contractile function during low-flow ischemia. Circulation. 2005; 111:906–12. [PubMed: 15699252]

[29]. Yuan C, Guo Y, Ravi R, Przyklenk K, Shilkofski N, Diez R, et al. Myosin binding protein C is differentially phosphorylated upon myocardial stunning in canine and rat hearts — evidence for novel phosphorylation sites. Proteomics. 2006; 6:4176–86. [PubMed: 16791825]

[30]. Sadayappan S, Osinska H, Klevitsky R, Lorenz JN, Sargent M, Molkentin JD, et al. Cardiac myosin binding protein C phosphorylation is cardioprotective. Proc Natl Acad Sci U S A. 2006; 103:16918–23. [PubMed: 17075052]

[31]. Sadayappan S, Gulick J, Osinska H, Martin LA, Hahn HS, Dorn GW, et al. Cardiac myosin-binding protein-C phosphorylation and cardiac function. Circ Res. 2005; 97:1156–63. [PubMed: 16224063]

[32]. Stelzer JE, Patel JR, Walker JW, Moss RL. Differential roles of cardiac myosin-binding protein C and cardiac troponin I in the myofibrillar force responses to protein kinase A phosphorylation. Circ Res. 2007; 101:503–11. [PubMed: 17641226]

[33]. Fukuda N, Wu Y, Nair P, Granzier HL. Phosphorylation of titin modulates passive stiffness of cardiac muscle in a titin isoform-dependent manner. J Gen Physiol. 2005; 125:257–71. [PubMed: 15738048]

[34]. Yamasaki R, Wu Y, McNabb M, Greaser M, Labeit S, Granzier H. Protein kinase A phosphorylates titin's cardiac-specific N2B domain and reduces passive tension in rat cardiac myocytes. Circ Res. 2002; 90:1181–8. [PubMed: 12065321]

[35]. Kruger M, Kotter S, Grutzner A, Lang P, Andresen C, Redfield MM, et al. Protein kinase G modulates human myocardial passive stiffness by phosphorylation of the titin springs. Circ Res. 2009; 104:87–94. [PubMed: 19023132]

[36]. Shah AM, Prendergast BD, Grocott-Mason R, Lewis MJ, Paulus WJ. The influence of endothelium-derived nitric oxide on myocardial contractile function. Int J Cardiol. 1995; 50:225–31. [PubMed: 8537145]

[37]. Layland J, Li JM, Shah AM. Role of cyclic GMP-dependent protein kinase in the contractile response to exogenous nitric oxide in rat cardiac myocytes. J Physiol. 2002; 540:457–67. [PubMed: 11956336]

[38]. Shah AM, Spurgeon HA, Sollott SJ, Talo A, Lakatta EG. 8-bromo-cGMP reduces the myofilament response to Ca2+ in intact cardiac myocytes. Circ Res. 1994; 74:970–8. [PubMed: 8156644]

[39]. Moens AL, Ketner EA, Takimoto E, Schmidt TS, O'Neill CA, Wolin MS, et al. Bi-modal dose-dependent cardiac response to tetrahydrobiopterin in pressure-overload induced hypertrophy and heart failure. J Mol Cell Cardiol. 2011; 51:564–9. [PubMed: 21645517]

[40]. Colson BA, Locher MR, Bekyarova T, Patel JR, Fitzsimons DP, Irving TC, et al. Differential roles of regulatory light chain and myosin binding protein-C phosphorylations in the modulation of cardiac force development. J Physiol. 2010; 588:981–93. [PubMed: 20123786]

[41]. Harris SP, Lyons RG, Bezold KL. In the thick of it: HCM-causing mutations in myosin binding proteins of the thick filament. Circ Res. 2011; 108:751–64. [PubMed: 21415409]

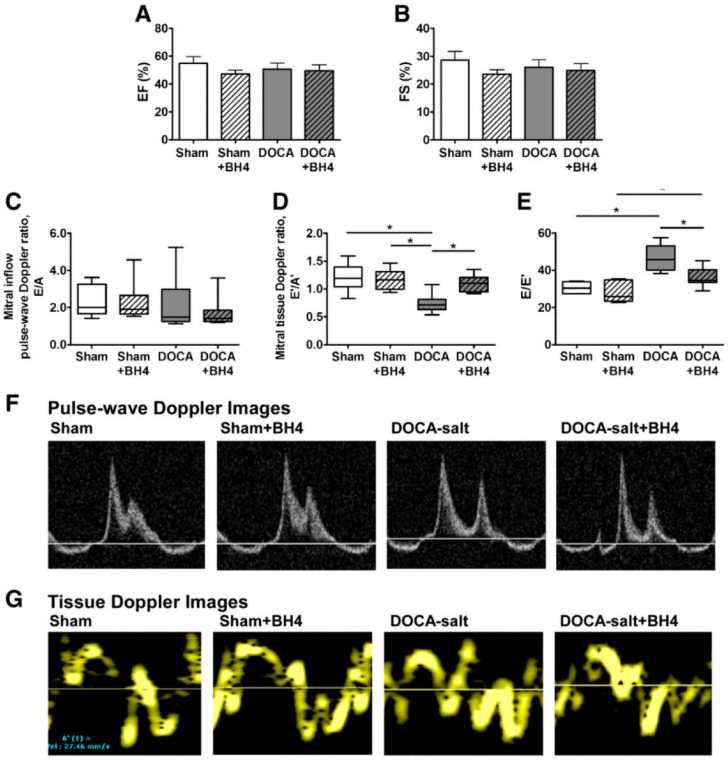

Fig. 1.

Thoractic echocargiographic parameters in WT and DOCA-salt mice treated with or without BH_4. (A) Ejection fraction (%, EF) and (B) fractional shortening (%, FS) were determined in short axix M-mode view. (C) Mitral inflow pulse-wave Doppler ratio (E/A). (D) Mitral tissue doppler ratio, E'/A'. (E) E/E'. (F–G), Representative images from apical four chamber view of pulse-wave (F) and TDI (G). Data was represented mean±SEM. N=7–9 per group. Data were statistically analyzed using JMP statistical software by two-way ANOVA followed by Student's *t*-test. **P*<0.05.

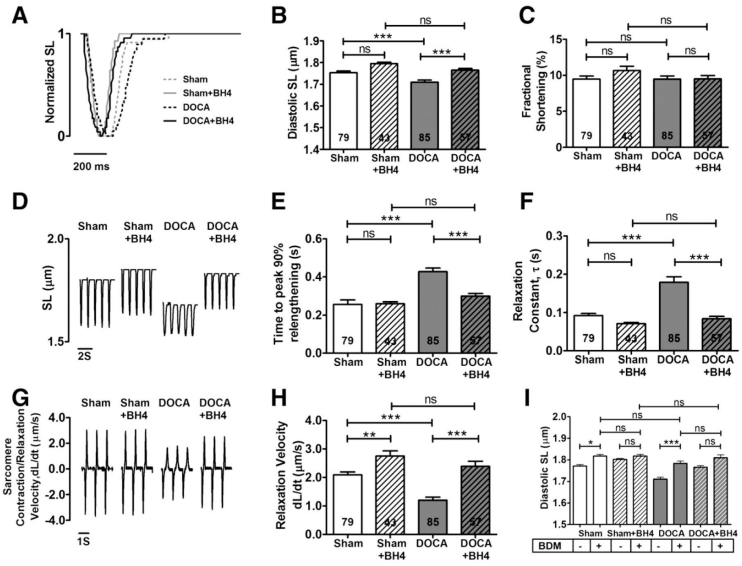

Fig. 2.

Improved diastolic sarcomere length and relaxation impairement by BH_4 treatment. Isolated myocytes from sham, sham+BH_4, DOCA-salt and DOCA-salt+BH_4 groups were stimulated at 1 Hz recorded by Ionoptix. (A) Normalized sarcomere trace. (B) Diastolic resting SL of DOCA-salt group was restored by BH_4 treated group. (C) Fractional shortening. (D) Sarcomere contraction and relaxation trace. (E) Peak 50% Relengthening time. (F) Relaxation constant, **τ**. (G) Sarcomere contraction/relaxation velocity trace. (H) Relaxation velocity. (I) BDM effect on sarcomere relaxations. BDM (10 mmole/L) was treated on isolated myocytes from Sham, Sham+BH_4, DOCA-salt, and DOCA-salt+BH_4 groups. DOCA-salt myocytes were increased residual SL by BDM, but there is no difference of residual SK between all groups after BDM treatment. Data was represented mean±SEM. Myocytes n number were indicated as accordingly from 5 to 7 mice per group. Data were statistically analyzed using JMP statistical software by two-way ANOVA followed by Student's *t*-test. **P*<0.05.

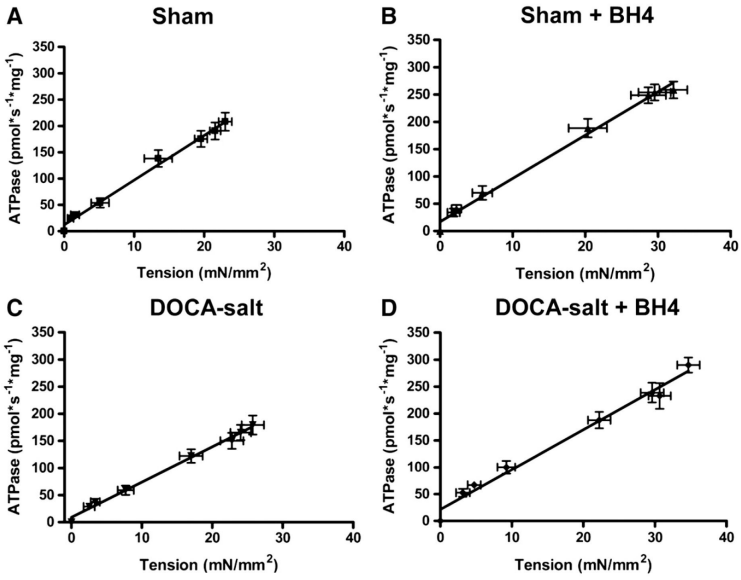

Fig. 3.

Tension cost for fibers from Sham (A), Sham+BH_4 (B), DOCA-salt (C), and DOCA-salt +BH_4 (D) groups. Data was represented mean±SEM. N=9–17 fibers per group.

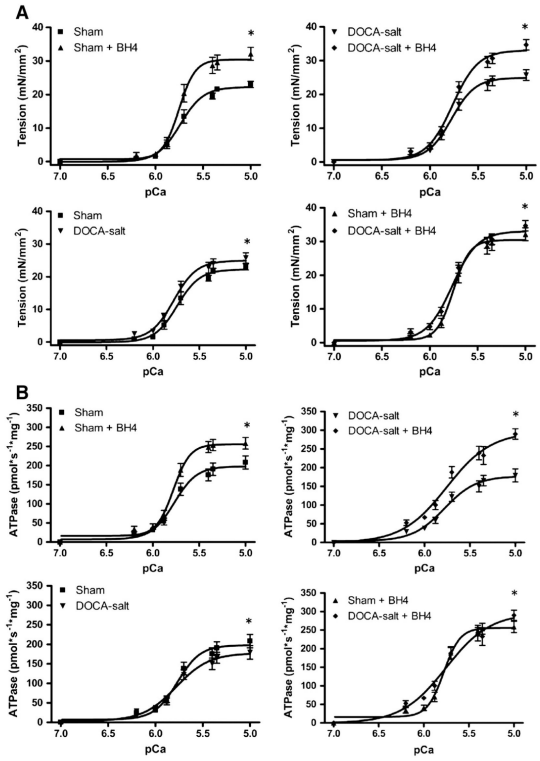

Fig. 4.

Ca^{2+}-sensitivity and ATPase of skinned fiber preparations. (A) Maximal tension and pCa_{50} for tension are increased in fibers from DOCA-salt group compared to Sham group. (B) Maximal ATPase increased in fibers from the DOCA-salt+BH_4 group compared to fibers from the DOCA-salt group. Data was represented mean±SEM. N=9–17 fibers per group. Data were statistically analyzed using JMP statistical software by two-way ANOVA followed by Student's *t*-test. **P*<0.05.

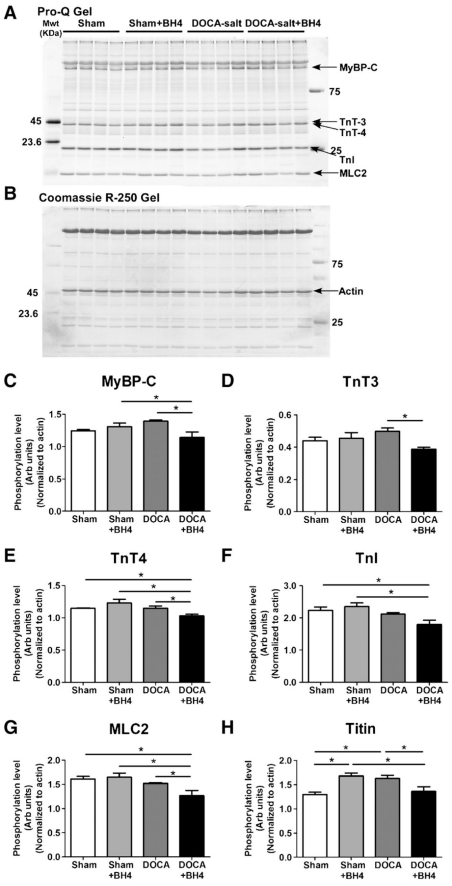

Fig. 5.

Phosphorylation levels of myofilaments proteins. (A) Representative ProQ and (B) Coomassie R-250 gel of skinned fiber myofibril proteins. (C–G) Phosphorylation levels of myofilament proteins as assessed by ProQ. (C) MyBP-C, (D) TnT3, (E) TnT4, (F) TnI, (G) MLC2, and (H) titin. Data were normalized to actin and statistically analyzed using JMP statistical software by two-way ANOVA followed by Student's *t*-test. N=4 mice per group.

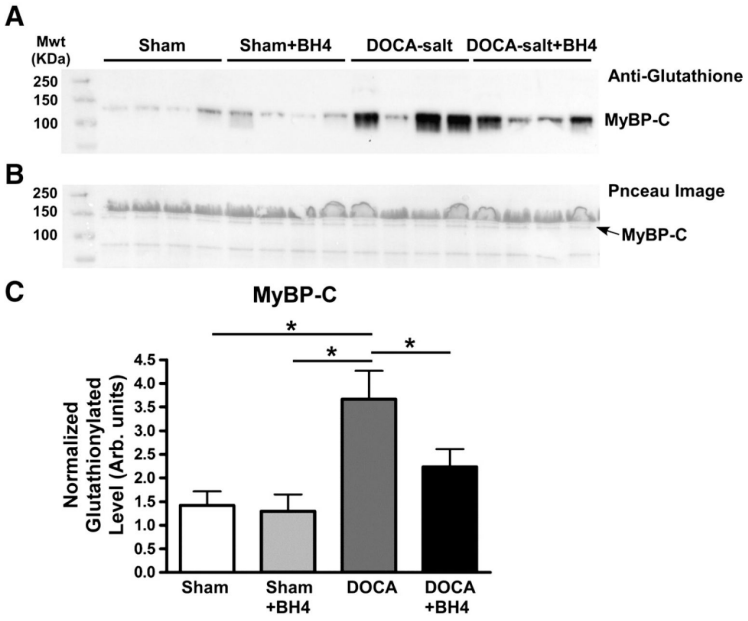

Fig. 6.

Glutathionylation levels of MyBP-C. (A) Representative anti-glutathione gel. (B) Representative ponceau image. (C) MyBP-C glutathionylation level normalized to total lane. Band densitometry data were represented mean±SEM. N=8 mice per group. Data were statistically analyzed using JMP statistical software by two-way ANOVA followed by Student's *t*-test. **P*<0.05.

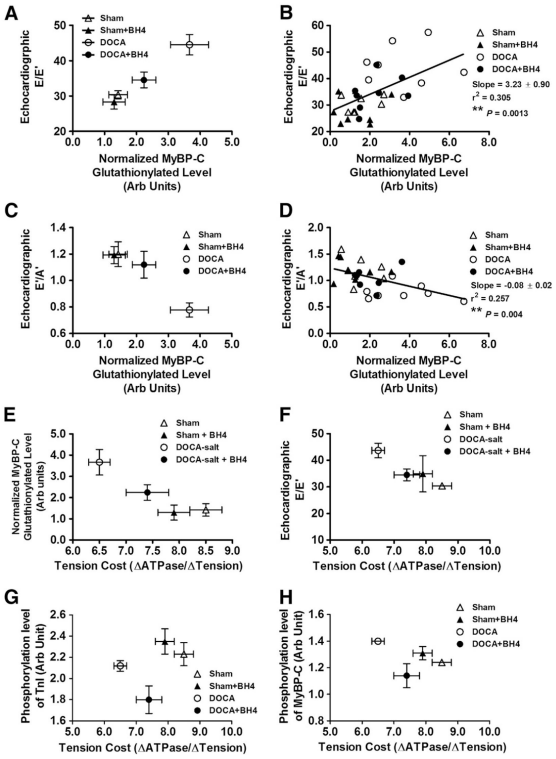

Fig. 7.

Relationship between MyBP-C glutathionylation, diastolic dysfunction, and tension cost. (A–B) Echocardiographic parameter, E/E' ratio was positively correlated with normalized MyBP-C glutathionylation level. (C–D) Echocardiographic parameter, E'/A' ratio was negatively correlated with normalized MyBP-C glutathionylation level. Tension cost vs. normalized MyBP-C glutathionylation level (E) and tension cost vs. echocardiographic E/E' (F) were negatively correlated. (G–H) Tension cost vs. phosphorylation level of TnI (G) and phosphorylation level of MyBP-C (H) from ProQ data. N=7–8 mice per group. * indicates linear regression ** $P<0.01$.

Table 1

Transthoracic echocardiography measurements in vivo BH_4 treatment in DOCA-salt mice.

	Sham	Sham+BH_4	DOCA-salt	DOCA-salt+BH_4
LV M-mode protocol				
EF (%)	56.3±3.9	51.1±2.8	51.9±4.4	54.5±5.0
FS (%)	28.9±2.8	24.7±1.6	26.4±2.7	26.6±2.9
LVESD (mm)	2.74±0.16	3.01±0.11	2.86±0.18	2.65±0.21
LVEDD (mm)	3.86±0.08	4.05±0.10†	3.87±0.11	3.67±0.14†
Mitral valve protocol				
MV E (mm/s)	698.2±35.9$^{\wedge}$	738.1±31.1$^{\dagger\&}$	613.7±45.8$^{\&}$	555.0±35.1$^{\dagger\wedge}$
MV A (mm/s)	326.8±30.1	357.5±31.7	329.2±48.7	367.8±48.3
MV E/A ratio	2.31±0.31	2.28±0.33	2.15±0.46	1.71±0.33
Tissue Doppler protocol				
E' (mm/s)	22.3±1.7$^{\wedge *}$	24.4±2.2$^{\dagger\&}$	14.3±0.8$^{\&*}$	16.8±1.3$^{\dagger\wedge}$
A' (mm/s)	19.4±1.9	21.1±1.9†	20.1±1.4‡	15.2±1.0†‡
E'/A' ratio	1.20±0.09*	1.17±0.06$^{\&}$	0.74±0.05$^{\ddagger *\&}$	1.12±0.10‡
E/E' ratio	30.38±1.17*	34.91±6.81$^{\&}$	43.69±2.73$^{*\&\ddagger}$	34.53±2.22‡
Sm	20.8±1.8	22.9±1.5†	18.5±1.6	15.8±1.5†

EF, ejection fraction; FS, fractional shortening; LVESD, left ventricle end systolic diameter; LVEDD, left ventricle end diastolic diameter;MV,mitral valve;MV E,mitral inflowvelocity peak early filing;MV A,mitral inflowvelocity peak late filing; E',mitral annulus longitudinal velocity tissue Doppler early filing rate; A' mitral annulus longitudinal velocity tissue Doppler late filing rate; Sm, mitral annulus longitudinal velocity tissue Doppler systolic velocity. Data are represented as mean±SEM (n=7–9 per group).

$^{\#}P$<0.05 for Sham vs. Sham+BH_4.

$^{*}P$<0.05 for Sham vs. DOCA-salt.

$^{\dagger}P$<0.05 for Sham+BH_4 vs. DOCA-salt+BH_4.

$^{\ddagger}P$<0.05 for DOCA-salt vs. DOCA-salt+BH_4.

$^{\wedge}P$<0.05 for Sham vs. DOCA-salt+BH_4.

$^{\&}P$<0.05 for Sham+BH_4 vs. DOCA-salt.

Table 2

Effect of BH_4 on tension and ATPase rate of skinned fiber bundles.

	Sham	Sham+BH_4	DOCA-salt	DOCA-salt+BH_4
Maximum ATPase (pmol·s^{-1}·mg^{-1})	197.8±2.3$^{\#*\wedge}$	256.0±1.7$^{\#\dagger}$	177.5±2.0*‡	296.0±4.7$^{\dagger\ddagger\wedge}$
pCa50 for tension	5.739±0.006$^{*\wedge}$	5.753±0.004	5.776±0.004*	5.766±0.005$^{\wedge}$
Maximum tension (mN/mm^2)	22.22±0.19$^{\#*\wedge}$	30.43±0.19$^{\#\dagger}$	24.92±0.15*‡	33.04±0.25$^{\dagger\ddagger\wedge}$
Tension cost ΔATPase/ΔTension	8.5±0.3*	7.9±0.3	6.5±0.2*‡	7.4±0.4‡

Data are means±SEM. N=9–17 fibers,

$^{\#}P<0.05$ for Sham vs. Sham+BH_4.

$^{*}P<0.05$ for Sham vs. DOCA-salt.

$^{\dagger}P<0.05$ for Sham+BH_4 vs. DOCA-salt+BH_4.

$^{\ddagger}P<0.05$ for DOCA-salt vs. DOCA-salt+BH_4.

$^{\wedge}P<0.05$ for Sham vs. DOCA-salt+BH_4.